Invertebrate Biology 127(4): 396–402.

DOI: 10.1111/j.1744-7410.2008.00143.x

Magnetic resonance imaging of live freshwater mussels (Unionidae)

F. Michael Holliman,[1,a] Denise Davis,[2] Arthur E. Bogan,[3] Thomas J. Kwak,[1,4] W. Gregory Cope,[5] and Jay F. Levine[6]

[1] NC Cooperative Fish and Wildlife Research Unit, Department of Zoology, NC State University, Raleigh, North Carolina 27695-7617, USA
[2] Magnetic Resonance Research Center, University of Pittsburgh Medical Center, Pittsburgh, Pennsylvania 15213, USA
[3] NC Museum of Natural Sciences, Raleigh, North Carolina 27601, USA
[4] US Geological Survey, Raleigh, North Carolina USA
[5] Department of Environmental and Molecular Toxicology, NC State University, Raleigh, North Carolina 27695-7633, USA
[6] College of Veterinary Medicine, NC State University, Raleigh, North Carolina 27606, USA

Abstract. We examined the soft tissues of live freshwater mussels, Eastern elliptio *Elliptio complanata,* via magnetic resonance imaging (MRI), acquiring data with a widely available human whole-body MRI system. Anatomical features depicted in the profile images included the foot, stomach, intestine, anterior and posterior adductor muscles, and pericardial cavity. Noteworthy observations on soft tissue morphology included a concentration of lipids at the most posterior aspect of the foot, the presence of hemolymph-filled fissures in the posterior adductor muscle, the presence of a relatively large hemolymph-filled sinus adjacent to the posterior adductor muscle (at the ventral-anterior aspect), and segmentation of the intestine (a diagnostic description not reported previously in Unionidae). Relatively little is known about the basic biology and ecological physiology of freshwater mussels. Traditional approaches for studying anatomy and tissue processes, and for measuring sub-lethal physiological stress, are destructive or invasive. Our study, the first to evaluate freshwater mussel soft tissues by MRI, clarifies the body plan of unionid mussels and demonstrates the efficacy of this technology for *in vivo* evaluation of the structure, function, and integrity of mussel soft tissues.

Additional key words: MRI, morphology, bivalve, soft tissue, unionid

North America supports the greatest diversity of freshwater mussels (Bivalvia: Unionidae) on the planet, ~300 of the 800 species known (Haas 1969, The Mussel Project: http://clade.acnatsci.org/mussel/index.html). The International Union for Conservation of Nature and Natural Resources (IUCN)-World Conservation Union recently placed 41% of the unionid species occurring in North America on the 2004 IUCN Red List, regarded as critically endangered, endangered, or vulnerable. Imperilment of this magnitude has global significance (Baillie et al. 2004).

The physiological ecology and basic biology, as well as the phylogeny, of many freshwater mussel species remain poorly understood, which may hinder conservation and recovery efforts (Baker & Hornbach 2001; Campbell et al. 2005). Traditional approaches for elucidating basic biology and health problems in freshwater mussels have required lethal sampling and dissection of specimens or invasive procedures, potentially jeopardizing survival of small populations. Thus, species most in need of additional study may receive the least attention from the scientific community to avoid population effects of research.

Magnetic resonance imaging (MRI) has demonstrated abilities for non-invasive assessment of soft tissue structure, integrity, and biochemistry in live organisms, becoming common in human clinical environments. MRI would appear to meet the needs of researchers working with freshwater bivalves as a means for non-destructive and non-invasive assessments of soft tissues, an especially important consideration when working with imperiled mussels. Increasingly, human MRI systems are adopted for use on companion animals (e.g., dog, cat) in veteri-

[a] Author for correspondence.
E-mail: fmholliman@yahoo.com

nary medicine (Walker 1995). Achievement of adequate signal to noise ratios (SNRs) and image resolution are challenges when using human MRI systems on small animals (e.g., mouse, rat); increased scan times (increasing expense) and/or specialized hardware may be necessary when imaging small animals with human MRI systems (Pfefferbaum et al. 2004). Whether the performance of a typical clinical human whole-body MRI system is adequate for the study of freshwater bivalves, animals of relatively small size, is not known.

Eastern elliptios (*Elliptio complanata* LIGHTFOOT 1786) are found in freshwater throughout the Atlantic slope of North America, are often used in studies evaluating the effects of exposure to toxicants, and as surrogates for imperiled species (e.g., Chittick et al. 2001). Thus, we selected the Eastern elliptio as the model species for our study. Data were acquired with a widely available clinical, human whole-body MRI system. Freely available software packages and typical computer systems were used for post-processing of images. We report on this first step in the development of MRI for widespread use on freshwater mussels.

Methods

Individuals of *Elliptio complanata* were collected from a small stream in central North Carolina and transported, moist and cool, in an ice chest with a dampened fabric to prevent direct contact between blue-ice packs and mussels (Cope et al. 2003). MRI was conducted on four adult mussels (maximum lengths: 64–77 mm; wet weights: 40–65 g) at the Magnetic Resonance Research Center, University of Pittsburgh Medical Center, Pittsburgh, PA, USA. Images were collected on one mussel known to have been gravid earlier in the season. An equal number of mussels designated as controls were transported and handled similarly to those undergoing MRI, but were not subjected to imaging. Imaging and transport were accomplished without anesthetics. After data collection, the mussels were transported to an indoor tank at the College of Veterinary Medicine, North Carolina State University, Raleigh, NC, USA, where survival was monitored for 30 d. The mussels were transported >1600 km (>1000 miles) over a period of 5 d.

Imaging system and protocol

Image data were acquired using a 127.4 MHz, 3-T horizontal bore, whole-body scanner (General Electric Medical Systems, Milwaukee, WI, USA). The cylindrical bore of the magnet was 92.5 cm and the gradient core was 60 cm (inner dimensions). Tissue excitation and signal reception were accomplished with a commercially available transceiver (volume 23 cm $\times$ 22 cm $\times$ 19.5 cm) typically used for the clinical MRI of human extremities. To alleviate concern that the mussels presented an inadequate filling ratio (volume of mussel to volume of the transceiver) and loading for the coil circuitry, which would result in insufficient SNR, the mussels were held in 0.5–1 L MRI-safe containers filled with distilled water during the data acquisition. Data were acquired on one mussel at a time with the mussel positioned on the left valve.

Data were acquired with spoiled gradient recalled (SPGR) and fast-spin echo dual-echo (FSE-DE) imaging sequences. Parameters for the SPGR imaging sequence (TR, 18 ms; TE, minimum; flip angle, 15°) were selected to acquire T1-weighted images (T1WIs). That is, signals associated with spin-lattice tissue relaxation (e.g., lipids and proteinaceous fluids) were enhanced in images acquired with the SPGR pulse sequence. The parameters of the FSE-DE pulse sequence (TR, 3000 ms; TE, 15, 102 ms, ETL, 8) were selected to produce interleaved hypo- and hyper-intense T2-weighted images (T2WIs), where weighting (contrast) in the hypo-intense images reflected relative proton density, and the signals from loosely bound protons (e.g., fluids) were enhanced in the hyper-intense images.

Low-resolution images (0.8 mm $\times$ 0.8 mm $\times$ 4 mm, 200 mm^2 field-of-view, 256 mm^2 matrix) acquired in three dimensions for survey of location showed soft tissue features were most recognizable in the sagittal plane. Thus, coordinates and directions for data collections were graphically defined to acquire sagittal profile images. The image profiles were aligned to the interior edges of the valves. The T1WIs were acquired at a resolution of 0.2 mm $\times$ 0.2 mm $\times$ 1 mm in a 512 mm^2 matrix. The T2WIs were acquired at 0.4 mm $\times$ 0.4 mm $\times$ 2 mm in a 256 mm^2 matrix, with 1 mm skipped between profiles. Data were acquired in a 100 mm^2 field-of-view with signal averaging set at 2. Acquisition time (min:s) was 10:30 for the T1WI and 6:30 for the T2WI. The MRI system was tuned for optimal performance (bandwidth of radiofrequencies transmitted, receiver gain, transmitter gain) before each imaging sequence.

Data processing and analysis

Data were transferred from the MRI system to compact disc for transport. Conversion of the data files from GE Signa to Analyze format (Mayo Foundation, Rochester, MN, USA) and image post-processing were accomplished on a personal computer using ImageJ

(Rasband WS 1997–2005, US National Institutes of Health, Bethesda, ML, USA; http://rsb.info.nih.gov/ij/) and MRIcro (Rorden & Brett 2000), freely available software packages. Identification of anatomic features in the images was aided by published figures of mussel anatomy (Burch 1975; McMahon & Bogan 2001) and gross dissections of fixed mussels (10% formalin) using stereo and digital microscopy.

Delineation of anatomic structures in the T1WIs and data extractions were accomplished by normalizing pixel intensities to range 0–255 and applying binary thresholds, edge detection algorithms, and subtraction processes. The delineations of the anatomical features are hereafter referred to as regions of interest (ROIs). SNRs were calculated for ROIs in the T1WIs as $SNR_{ROI} = \text{mean } SI_{ROI}/\text{STDV Noise}_{ROI}$, where SI is the signal intensity and Noise was non-object noise within a $1\,cm^2$ ROI. Contrast-to-noise ratios (CNRs) were estimated as $CNR = SNR_{ROI} - SNR_{WaterROI}$, the difference in SNR between tissue ROI and a $1\,cm^2$ ROI in environmental water. The CNRs were used for comparison of relative responses among the various tissues. The SNRs and CNRs of the various tissue features were estimated for each profile. The mean CNRs and 95% confidence intervals (95% CI) are reported. The volumes (mm^3) of the anatomical features depicted in the T1WIs were estimated by summing the areas (mm^2) of the ROIs.

The T2 responses of the tissues were compared between the dual-echo series using identical ROIs. The SI distributions of the various tissues were summarized in side-by-side box-and-whisker plots, where the first, second, and third quartiles of the data were represented by the horizontal lines of the boxes, the upper and lowermost SI values within $1.5\times$ the interquartile range were represented by whiskers (McGill et al. 1978). The data analysis for this article was generated using SAS/STAT software, version 9.1 of the SAS System (SAS Inc., Cary, NC, USA) for personal computers.

Results

The soft tissues of the mussels were depicted in the image profiles, in their entirety (Fig. 1). The gross anatomy depicted in the images was consistent among the mussels. Image resolution, gray scale, and textures permitted identification of the foot, anterior adductor muscle, stomach, intestine, posterior pedal retractor, pericardial cavity, and the posterior adductor muscle (Fig. 2). Gill and mantle tissues were visible, but not consistently. The CNRs in the T1WI sequences varied ~11–14, indicating a marked difference in spin-lattice relaxation in the mussel tissues and the environmental water used for reference. There was good agreement in the relative SI of the various tissue features among the mussels, and a consistent relationship between relative SI and tissue type. CNRs in the T1WIs were greatest in the foot and anterior adductor muscle and least in the pericardial cavity and the intestine (Fig. 3). In each of the mussels, the SI was greatest at the most posterior aspect of the foot (Fig. 2), an indication of increased lipid concentration relative to other regions. The total volumes of the soft tissues, estimated from the T1WI, of the mussels were 7,924, 12,294, and $18{,}169\,mm^3$ (Table 1). In each of the mussels, the tissues of the greatest volume were the visceral mass complex, the foot, and the posterior adductor muscle.

In most cases, identification of anatomic features and segmentation in the T1WIs were aided by regions with relatively low SI, for example, relative reduction in SI immediately adjacent to the stomach and intestine, as well as other tissues in the central region of the visceral mass. SI of this tissue was relatively low in both T1WI (Fig. 2) and T2WI (Fig. 4). The SI from the hemolymph was enhanced in the T2WI. The SI distributions associated with the various anatomic features depicted in the images shifted between the two echo times (15 and 102 ms) in the T2WIs (Fig. 5). Heterogeneity in the SI distributions was apparent among the tissue types, in the T2WIs.

The T1WIs and the T2WIs provided valuable morphologic information on the soft tissues. The shape of the intestine was elaborate, and consistent among the mussels, with descending, ascending, and transverse segments, traveling in dorsal, ventral and side-to-side directions, and doubling back on itself twice. The section of the intestine proximal to the junction with the pericardial region increased in size markedly in each of the mussels (Figs. 1 and 2). Examination of the region of the gonad failed to detect differences in appearance between the mussel known to have been gravid and those that were not. The SI in anatomic features, expected to be hemolymph filled (e.g., the region of the heart), was reduced in the T1WIs. Conversely, signals were enhanced in anatomical regions that were expected to be filled with hemolymph, in the T2WIs. Longitudinal fissures, filled with hemolymph, were apparent in the posterior adductor muscle (Fig. 4). Similarly, a hemolymph-filled sinus was apparent on the ventral-anterior aspect of the posterior adductor muscle. The greatest SI in the hypo- and hyper-intense T2WIs occurred in these two regions, indicating the greatest concentrations of relatively mobile hydrogen (^1H) nuclei. Gill and mantle tissues were more apparent in the T2WI than in the T1WI. All mussels transported in the study survived the 30-d post-imaging observation period.

Fig. 1. High-resolution (0.2 mm × 0.2 mm × 1 mm) T1-weighted magnetic resonance imaging profiles demonstrating the soft tissues in an individual of *Elliptio complanata* (scale bar [upper left] = 10 mm).

Discussion

Our results demonstrate that freshwater mussel soft tissues can be evaluated *in vivo* with a typical human MR scanner. Adequate image resolution and contrast were achieved without specialized coils, software, or excessive scan time. Although *Elliptio complanata* was the unionid evaluated in the present study, it is likely that the technique will transfer directly to other freshwater mussel species of similar size.

The vital parameters for assessing the health of freshwater bivalves remain largely unknown. Death is still the end-point for many freshwater bivalve health assessments whether for conservation or for quantification of risks associated with contaminant exposure (Patterson et al. 1999; Chittick et al. 2001). Ironically, energy analyses (lipids) to establish physiological health may involve killing the animals under investigation (Baker & Hornbach 2000). Biochemical evaluations of small tissue samples collected via biopsy can be used in evaluations of freshwater mussel health (Naimo et al. 1998). Although non-lethal, biopsy is an invasive procedure and could pose unacceptable risks to mussel survival (e.g., pathogens). The signals emitted by tissues during MRI are indicative of tissue biochemistry and can be collected non-invasively and non-destructively, an important consideration for working with imperiled mussels.

Contrasts in MR images reflect differences in proton density and biologically determined tissue relaxation rates (T1 and T2). It is the molecular environment of tissues that determines the T1 and T2 relaxation rates. Our study focused on MR signals emitted by ^{1}H nuclei. The MR signals produced by closely bound hydrogen (e.g., those of fats, lipids, and proteinaceous fluids) are distinguishable from those produced by less tightly bound protons (e.g., the fluids in extra- and intracellular spaces) and those of more mobile hydrogen nuclei (e.g., freely flowing biological fluids) (Pautler 2004).

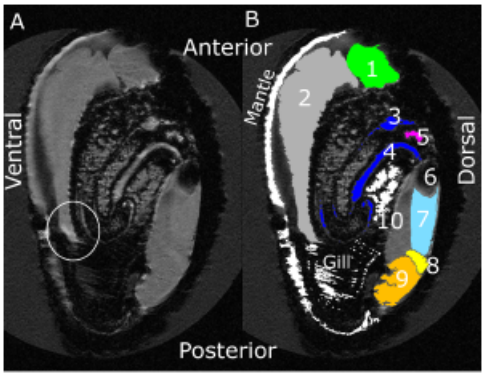

Fig. 2. **A.** Sagittal plane T1-weighted profile of an individual of *Elliptio complanata*. **B.** The same image after processing to remove the shell, external water, air artifacts, and segmentation of anatomical features. The features shown are the (1) anterior adductor muscle, (2) foot, (3) stomach, (4) gut or intestine, (5) digestive gland, (6) heart, (7) pericardial cavity, (8) pedal retractor, (9) posterior adductor muscle, and (10) tissues of the visceral mass. The circle indicates the tissues having the greatest signal intensities.

An index of mussel health attained non-invasively and non-destructively that can be repeated on the same animal would be an especially powerful tool, useful for monitoring individuals and populations through longitudinal studies. Changes in tissue relaxation rates are often associated with pathology (Pautler 2004). In the clinical environment, T2WIs similar to those acquired in our study are often used for evaluation of increased intra- or extra-cellular water, indications of edema, or various pathologies. Tissue-specific accumulation of stress proteins, in response to contaminant exposure,

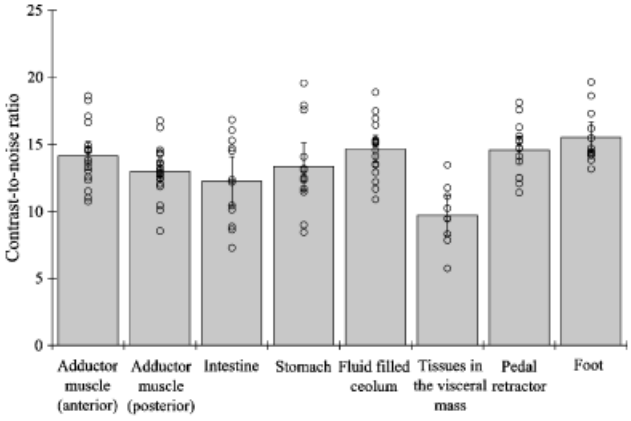

Fig. 3. Estimated mean and 95% confidence intervals (error bars) for contrast-to-noise ratios (CNRs) for various tissues depicted in the T1WI images, referenced to environmental water. Signals from hydrogen nuclei associated with fats and lipids were enhanced in these images. Point estimates of CNRs from the individual image profiles are provided.

Table 1. Voxel volumes (mm^3) of all tissues and of the primary anatomic structures of three live mussels. Volumes were estimated from T1-weighted magnetic resonance images.

	Volume (mm^3)		
	Mussel ID		
Anatomical feature	One	Two	Three
All tissues	7,924	12,294	18,169
Visceral mass complex	1,690	1,990	3,537
Visceral mass tissues	745	245	348
Gut	216	165	328
Foot	1,793	1,575	1,618
Posterior adductor muscle	945	894	1,514
Anterior adductor muscle	486	363	1,002

has been reported in blue mussel (*Mytilus edulis* Linnaeus 1758) (Tedengren et al. 2004), a condition likely to be detected with MRI. Signals from lipids are enhanced in T1-weighted MR images, a potential basis for energy evaluations. The most posterior aspect of the foot appears lipid rich compared with the other tissues in *E. complanata,* a finding useful for both localizing lipid concentration and a demonstration of the potential of MRI for quantifying the physiological condition. The estimates of tissue volume in our study, derived from signals emitted by closely bound protons (e.g., lipids), demonstrate the potential for morphometric assessments (e.g., shape, volume, relative distance between structures) related to health and phylogeny. Further investigation into associations between MRI data and mussel physiological condition, pathology, and effects of contaminant exposure, as well as comparative study among species, is warranted.

The results of our study increase understanding of soft tissue morphology in the Unionidae. Segmentation of the intestine was demonstrated in each of the mussels in our study, a soft tissue characteristic reported in the Mycetopodidae of South America (Mansur 1974; Simone 1994), but not documented previously in the Unionidae of North America. The circulatory system in the Unionidae is characterized as open, the circulatory fluid flowing through sinuses (McMahon & Bogan 2001) rather than a network of vessels. Conservation efforts have been aided by the recent development of an invasive, but non-lethal technique, for hemolymph extraction from adductor muscles (Gustafson et al. 2005a,b). Images acquired in our study provide evidence of hemolymph-filled fissures within the adductor muscles. Perhaps more importantly, we demonstrate a relatively large hemolymph-filled sinus adjacent to the posterior adductor muscle. The hemolymph-filled sinus

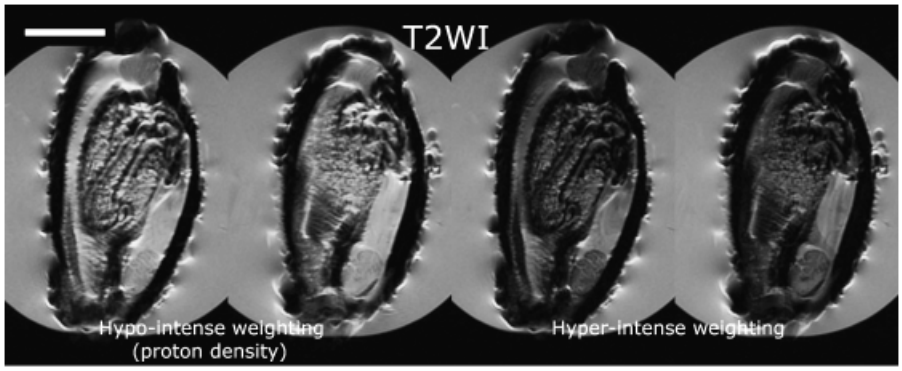

Fig. 4. Low-resolution hypo- and hyper-intense T2-weighted (T2W) images of individuals of *Elliptio complanata*. Distributions of signal intensities within various anatomic features are represented by box-and-whisker plots. Note the presence of hemolymph-filled fissures in the posterior adductor muscle and the hemolymph-filled sinus adjacent to the posterior adductor muscle (scale bar [upper left] = 10mm).

may be a suitable site for extraction of hemolymph, although further study is warranted.

Our study completes a necessary first step in developing MRI for testing scientific hypotheses related to freshwater mussel biology and sub-lethal indicators of physiological stress associated with pathology and exposure to contaminants (e.g., cadmium, pesticides). MRI is a non-invasive, non-lethal tool that may be used to study freshwater mussel biology and health, capable of addressing hypotheses previously not possible. Whole-body MRI systems are widely available in human clinical environments and increasingly are available in animal medicine. The non-destructive and non-invasive qualities of MRI and the ability for mussels to be transported without excessive mortality (e.g., Cope et al. 2003) could provide a means to evaluate imperiled animals. Furthermore, data collected with MRI can be used to create data libraries, permanent records of the forms and functioning of animals remaining in this fauna threatened with extinction.

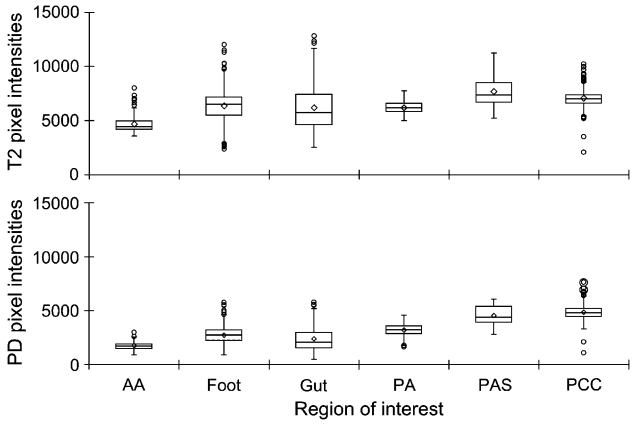

Fig. 5. Modified box-and-whisker plots of pixel intensities of the various anatomic features (regions of interest) in the proton density (PD) and T2-weighted images (i.e., hypo- and hyperintense T2WIs) of Eastern elliptio. Horizontal lines in the boxes represent the first, second, and third quartiles. The whiskers show the range of values falling within 1.5 × the inter-quartile range (IQR); values falling outside 1.5 × IQR are indicated by ○. The ◇ symbols within the boxes indicate mean values for the data distributions. AA, anterior adductor muscle; PA, posterior adductor cavity; PAS, posterior adductor sinus; PCC, pericardial cavity.

The cost of research-oriented MRI varies among facilities, but charges are based on usage time, typically ranging $100–$600 per hour. The total scan time for acquiring a series of images is influenced by the imaging sequences (programs) and parameter values (e.g., TR, matrix, number of signal averages, flip angle) used, where program and parameter selection is based on trade-offs between image contrast, resolution, SNR, and scan time. Furthermore, for a given imaging program and set of parameters, scan time scales inversely with magnet strength (Westbrook & Kaut 1993). In our study, we acquired the T1WI in 10:30 (min:s) and the T2WI (hypo- and hyper-intense weighting) in 6:30. We conclude that with refinement of the imaging parameters, these series can be acquired at a rate of four mussels per hour. Depending on the research objectives, all three series of images (T1WI, hypo-, hyper-intense T2WI) may not be desired, or resolution can be reduced, reducing expense. Development of protocols for imaging multiple mussels simultaneously would decrease the costs significantly.

Small animal MRI systems, and human MRI systems outfitted with specialized hardware for small animal imaging, can provide images of greater resolution than those acquired in our study (Pfefferbaum et al. 2004). Depending on the research goals, use of dedicated small animal MRI systems or use of specialized small animal hardware on human MRI systems may

be warranted. In comparison with typical human MRI systems, dedicated small animal MRI systems and human MRI systems with specialized small animal accoutrements are limited in availability. Our study demonstrates the efficacy of a typical human MRI system for evaluation of soft tissues in live freshwater mussels.

Acknowledgments. Dr. H. Michael Gach, University of Pittsburgh Medical Center, Magnetic Resonance Imaging Center, provided insight into parameter selection for the imaging sequences. Chris Eads, Paul Herbert, and Erin Shubert aided collection of mussels. Cynthia M. Bogan reviewed and commented on a draft of this article. We are grateful to two anonymous reviewers for their comments and suggestions; their efforts greatly improved this manuscript.

References

Baillie JEM, Bennun LA, Brooks TM, Butchart SHM, Chanson JS, Cokeliss Z, Hilton-Taylor C, Hoffmann M, Mace GM, Mainka SA, Pollock CM, Rodrigues ASL, Stattersfield AJ, & Stuart SN 2004. Globally threatened species. In: 2004 IUCN Red List of Threatened Species: A Global Species Assessment. Baillie JEM, Hilton-Taylor C, & Stuart SN, eds., pp. 25–26. Gland, Switzerland.

Baker SM. & Hornbach DJ 2000. Physiological status and biochemical composition of a natural population of unionid mussels (*Amblema plicata*) infested by zebra mussels (*Dreissena polymorpha*). Am. Midl. Nat. 143: 443–452.

——— 2001. Seasonal metabolism and biochemical composition of two unionid mussels, *Actinonaias ligamentina* and *Amblema plicata*. J. Moll. Stud. 67: 407–416.

Burch JB 1975. Freshwater Unionacean Clams (Mollusca: Pelecypoda) of North America. Malacological Publications, Hamburg, Germany.

Campbell DC, Serb JM, Buhay JE, Roe KJ, Minton RL, & Lydeard C 2005. Phylogeny of North American amblemines (Bivalvia, Unionoida): prodigious polyphyly proves pervasive across genera. Invertebr. Biol. 124: 131–164.

Chittick B, Stoskopf M, Law M, Overstreet R, & Levine J 2001. Evaluation of potential health risks to Eastern Elliptio (*Elliptio complanata*) (Mollusca: Bivalvia: Unionidae) and implications for sympatric endangered freshwater mussel species. J. Aquat. Ecosyst. Stress Rec. 9: 35–42.

Cope WG, Hove MC, Waller DL, Hornbach DJ, Bartsch MR, Cunningham LA, Dunn HL, & Kapuscinski AR 2003. Evaluation of relocation of unionid mussels to in situ refugia. J. Moll. Stud. 69: 27–34.

Gustafson LL, Stoskopf MK, Bogan AE, Showers W, Kwak TJ, Hanlon S, & Levine JF 2005a. Evaluation of a nonlethal technique for hemolymph collection in *Elliptio complanata,* a freshwater bivalve (Mollusca: Unionidae). Dis. Aquat. Organ. 65: 159–165.

Gustafson LL, Stoskopf MK, Showers W, Cope G, Eads C, Linnehan R, Kwak TJ, Andersen B, & Levine JF 2005b. Reference ranges for hemolymph chemistries from *Elliptio complanata* of North Carolina. Dis. Aquat. Organ. 65: 167–176.

Haas F 1969. Superfamily Unionacea. In: Treatise on Invertebrate Paleontology, Part N, Mollusca, 6. Vol. 1: Bivalvia. Moore RC, ed., pp. N411–N470. Geological Society of America and University of Kansas Press, Lawrence, KS, USA.

Mansur MCD 1974. *Monocondylaea minuana* Orbigny, 1835: variabilidade da Conchae Morfologia do Sistema Digestivo (Bivalvia, Mycetopodidae). Revista Iheringia Série Zoologia 45: 3–25.

Mcgill R, Tukey JW, & Larsen WA 1978. Variations of box plots. Am. Stat. 32: 12–16.

McMahon RF & Bogan AE 2001. Mollusca: Bivalvia. In: Ecology and Classification of North American Freshwater Invertebrates, 2nd ed. Thorp JH & Covich AP, eds., pp. 331–429. Academic Press, San Diego, CA, USA.

Naimo TJ, Damschen ED, Rada RG, & Monroe EM 1998. Nonlethal evaluation of the physiological health of unionid mussels: methods for biopsy and glycogen analysis. J. North Am. Benthol. Soc. 17: 121–128.

Patterson MA, Parker BC, & Neves RJ 1999. Glycogen concentration in the mantle tissue of freshwater mussels (Bivalvia: Unionidae) during starvation and controlled feeding. Am. Malacol. Bull. 15: 47–50.

Pautler RG 2004. Mouse MRI: concepts and applications in physiology. Physiology 19: 168–175.

Pfefferbaum A, Adalsteinsson E, & Sullivan EV 2004. *In vivo* structural imaging of the rat brain with a 3-T clinical human scanner. J. Magn. Reson. Imaging 20: 779–785.

Rorden C & Brett M 2000. Stereotaxic display of brain lesions. Behav. Neurol. 12: 191–200.

Simone LRL 1994. Anatomical characters and systematics of *Anodontites trapesialis* (Lamarck, 1819) from South America (Mollusca, Bivalvia, Unionoida, Muteloidea). Stud. Neotrop. Fauna Environ. 29: 169–185.

Tedengren M, Olsson B, Bradley BP, Gilek M, Reimer O, & Shepard JL 2004. Physiological and proteomic responses in *Mytilus edulis* exposed to PCBs and PAHs extracted from Baltic Sea sediments. Hydrobiologia 514: 15–27.

Walker M 1995. Introduction to magnetic-resonance-imaging in veterinary-medicine. Vet. Med. 90: 968–974.

Westbrook C & Kaut C 1993. MRI in Practice. Blackwell Scientific, Oxford, UK.